Research Articles: Neurobiology of Disease

Positive allosteric modulation as a potential therapeutic strategy in anti-NMDA receptor encephalitis

Natasha Warikoo¹, Samuel J. Brunwasser^{1,7}, Ann Benz¹, Hong-Jin Shu¹, Steven M. Paul^{1,2,3,6}, Michael Lewis², James Doherty², Michael Quick², Laura Piccio⁴, Charles F. Zorumski^{1,5,6}, Gregory S. Day^{4,8} and Steven Mennerick^{1,5,6}

DOI: 10.1523/JNEUROSCI.3377-17.2018

Received: 29 November 2017

Revised: 22 January 2018

Accepted: 12 February 2018

Published: 23 February 2018

Author contributions: N.W., S.P., M.L., J.J.D., M.Q., C.F.Z., G.S.D., and S.J.M. designed research; N.W., S.B., A.M.B., H.-J.S., and S.J.M. performed research; N.W., L.P., C.F.Z., G.S.D., and S.J.M. wrote the paper; S.B. and S.J.M. analyzed data; L.P. and G.S.D. contributed unpublished reagents/analytic tools.

Conflict of Interest: The authors declare no competing financial interests.

This work was funded by a sponsored project agreement between Sage Pharmaceuticals and Washington University School of Medicine. We thank Roberto Malinow and Elias Aizenman for making SEP-tagged and WT GluN subunits available and Anne Cross for help in obtaining control patient samples. Laura Piccio was supported by the Harry Weaver Neuroscience Scholar of the National Multiple Sclerosis Society (NMSS, JF 2144A2/1).

Correspondence: Steven Mennerick, Ph.D., Washington University School of Medicine, Department of Psychiatry, 660 S. Euclid Ave., Campus Box 8134, St. Louis, MO 63110, (314) 747-2988, menneris@wustl.edu

Cite as: J. Neurosci; 10.1523/JNEUROSCI.3377-17.2018

Alerts: Sign up at www.jneurosci.org/cgi/alerts to receive customized email alerts when the fully formatted version of this article is published.

Accepted manuscripts are peer-reviewed but have not been through the copyediting, formatting, or proofreading process.

¹Department of Psychiatry, Washington University School of Medicine

²Sage Therapeutics

³Voyager Therapeutics

⁴Department of Neurology, Washington University School of Medicine

⁵Department of Neuroscience

⁶Taylor Family Institute for Innovative Psychiatric Research, Washington University School of Medicine

⁷Medical Scientist Training Program, Washington University School of Medicine

⁸Knight Alzheimer Disease Research Center, Washington University School of Medicine

42

43

1	Positive allosteric modulation as a potential therapeutic strategy in anti-NMDA receptor
2	encephalitis
3	17
4	Natasha Warikoo ¹ , Samuel J. Brunwasser ^{1,7} , Ann Benz ¹ , Hong-Jin Shu ¹ , Steven M. Paul ^{1,2,3,6} ,
5	Michael Lewis ² , James Doherty ² , Michael Quick ² , Laura Piccio ⁴ , Charles F. Zorumski ^{1,5,6} ,
6	Gregory S. Day ^{4,8} , Steven Mennerick ^{1,5,6}
7	
8	Department of Psychiatry, Washington University School of Medicine
9	² Sage Therapeutics
10	³ Voyager Therapeutics
11	⁴ Department of Neurology, Washington University School of Medicine
12	⁵ Department of Neuroscience
13	⁶ Taylor Family Institute for Innovative Psychiatric Research, Washington University School of
14	Medicine
15	Medical Scientist Training Program, Washington University School of Medicine
16	⁸ Knight Alzheimer Disease Research Center, Washington University School of Medicine
17	
18	Abbreviated title: Anti-NMDAR therapeutic strategy
19	
20	Pages: 33
21	Figures: 8
22	Abstract words: 229
23	Introduction words: 371
24	Discussion words: 1219
25	
26	Correspondence to:
27	Steven Mennerick, Ph.D.
28	Washington University School of Medicine
29	Department of Psychiatry
30	660 S. Euclid Ave., Campus Box 8134
31	St. Louis, MO 63110
32	(314) 747-2988
33	menneris@wustl.edu
34	
35	Conflicts. Steven M. Paul, Michael Lewis, James Doherty, Michael Quick, and Charles F.
36	Zorumski have financial interests in Sage Therapeutics.
37	
38	Acknowledgements. This work was funded by a sponsored project agreement between Sage
39	Pharmaceuticals and Washington University School of Medicine. We thank Roberto Malinow
40	and Elias Aizenman for making SEP-tagged and WT GluN subunits available and Anne Cross

for help in obtaining control patient samples. Laura Piccio was supported by the Harry Weaver

Neuroscience Scholar of the National Multiple Sclerosis Society (NMSS, JF 2144A2/1).

44 ABSTRACT

45 N-methyl-D-aspartate receptors (NMDARs) are ionotropic glutamate receptors important for 46 synaptic plasticity, memory, and neuropsychiatric health. NMDAR hypofunction contributes to 47 multiple disorders, including anti-NMDAR encephalitis (NMDARE), an autoimmune disease of 48 the central nervous system associated with GluN1 antibody-mediated NMDAR internalization. 49 Here we characterize the functional/pharmacological consequences of exposure to cerebrospinal 50 fluid (CSF) from female human NMDARE patients on NMDAR function, and we characterize 51 the effects of intervention with recently described positive allosteric modulators (PAMs) of 52 NMDARs. Incubation (48 h) of rat hippocampal neurons of both sexes in confirmed NMDARE 53 patient CSF, but not control CSF, attenuated NMDA-induced current. Residual NMDAR 54 function was characterized by lack of change in channel open probability, indiscriminate loss of 55 synaptic and extrasynaptic NMDARs, and indiscriminate loss of GluN2B-containing and 56 GluN2B-lacking NMDARs. NMDARs tagged with N-terminal pHluorin fluorescence 57 demonstrated loss of surface receptors. Thus, function of residual NMDARs following CSF 58 exposure was indistinguishable from baseline, and deficits appear wholly accounted for by receptor loss. Co-application of CSF and PAMs of NMDARs (SGE-301 or SGE-550, oxysterol-59 60 mimetic) for 24 h restored NMDAR function following 24 h incubation in patient CSF. 61 Curiously, restoration of NMDAR function was observed despite wash-out of PAMs prior to 62 electrophysiological recordings. Subsequent experiments suggested that residual allosteric 63 potentiation of NMDAR function explained the persistent rescue. Further studies of the pathogenesis of NMDARE and intervention with PAMs may inform new treatments for 64 65 NMDARE and other disorders associated with NMDAR hypofunction.

67	Significance statement: Anti-N-methyl-D-aspartate receptor encephalitis (NMDARE) is
68	increasingly recognized as an important cause of sudden-onset psychosis and other
69	neuropsychiatric symptoms. Current treatment leaves unmet medical need. Here we demonstrate
70	cellular evidence that newly identified positive allosteric modulators of NMDAR function may
71	be a viable therapeutic strategy.
72	

INTRODUCTION

73

74 Anti-N-methyl-D-aspartate receptor encephalitis (NMDARE) is increasingly recognized as a 75 cause of sudden-onset psychosis and other neuropsychiatric symptoms (Fischer et al., 2016; 76 Dalmau et al., 2017). In fact, NMDARE is now reported as the most common cause of 77 autoimmune encephalitis, with comparable incidence and prevalence to infectious encephalitis 78 (Gable et al., 2012; Dubey et al., 2018). Indicated treatment for NMDARE includes 79 immunosuppressive therapies. With current treatment, approximately 80% of patients improve, 80 while relapses are reported in 14-25% of cases (Gabilondo et al., 2011; Titulaer et al., 2013). 81 Although reassuring, documented improvement may take place over protracted periods (Titulaer 82 et al., 2013), with persistent psychiatric and cognitive sequelae of disease increasingly 83 recognized (Finke et al., 2016). These findings emphasize the need for complementary 84 approaches to treatment (Panzer and Lynch, 2013), including interventions capable of mitigating 85 symptoms during the acute phase of disease, and strategies that promote receptor recovery and 86 improve longer-term outcomes. 87 At the cellular level, binding of NMDAR antibodies leads to capping and cross-linking of 88 NMDARs, resulting in receptor dimerization and internalization (Hughes et al., 2010). Other 89 90 results suggest that human NMDAR antibodies may alter surface NMDAR retention at synapses 91 (Mikasova et al., 2012). The combined effects are thought to be responsible for the unique 92 manifestations of signs and symptoms that characterize patients with NMDARE, a hypothesis 93 reinforced by the observation that several clinical features are reproduced with pharmacological 94 blockade of NMDARs (Krystal et al., 2002; Anticevic et al., 2012; Zorumski et al., 2016).

95	Although loss of surface receptors is key to antibody effects, whether remaining surface
96	receptors exhibit altered function because of antibody binding is unclear.
97	
98	We examined additional effects of NMDAR antibody exposure by challenging primary cultures
99	of rodent hippocampal neurons through incubation with cerebrospinal fluid (CSF) from
100	NMDARE patients. We found no evidence of altered function of remaining surface NMDARs
101	following 24-48 h of CSF exposure, nor preferential loss of synaptic versus extrasynaptic
102	NMDARS or GluN2A versus GluN2B-containing NMDARs. We provide proof-of-concept, in
103	vitro evidence that a class of oxysterol mimetics, selective positive allosteric modulators (PAMs)
104	of NMDAR function (Paul et al., 2013), rescue the effect of patient CSF when administered mid-
105	course of a 48 h incubation. The results implicate a novel drug class for rapid intervention in
106	NMDARE.
107	
108	MATERIALS AND METHODS
109	Hippocampal Cell Culture: Rat hippocampal neuron-astrocyte co-cultures were created and
110	maintained as previously described (Mennerick et al., 1995; Moulder et al., 2007; Emnett et al.,
111	2013) Briefly, hippocampi and cortical (astrocyte) tissue were dissected from PND 0-3 rats of
112	either sex using protocols approved by the Institutional Animal Care and Use Committee
113	(IACUC). Cells were seeded in modified Eagle's medium (Life Technologies) containing 5%
114	horse serum, 5% fetal calf serum, 17 mM D-glucose, 400 mM glutamine, 50 U/ml penicillin, and
115	50 mg/ml streptomycin. Mass cultures were plated at 650 cells/mm onto 25-mm cover glasses
116	coated with 5 mg/ml collagen or 0.1 mg/ml poly-D-lysine with 1 mg/ml laminin. Microisland
117	cultures were seeded on microdots of collagen on 0.15% agarose background as described

130

131

132

133

134

135

136

137

138

139

140

118 (Mennerick et al., 1995; Moulder et al., 2007; Emnett et al., 2013). Experiments were performed 119 at 7-11 DIV. 120 121 Patient material: CSF was collected from patients admitted to Barnes-Jewish Hospital 122 (Washington University in St. Louis; Saint Louis, Missouri) with definite autoimmune 123 encephalitis, including symptoms and signs consistent with NMDARE (Titulaer et al., 2013), and 124 antibodies against the GluN1 subunit of the NMDAR (clinical testing performed by the Mayo 125 Clinic; Rochester, Minnesota). The clinical assay for NMDARE is a cell-based assay using 126 specific anti-IgG immunofluorescence detection methods on transfected cells (EUROIMMUN, 127 Lübeck, Germany). We confirmed with anti-human IgG staining of tissue, as described below. 128

Patient A also presented with ovarian teratoma, a classic co-morbidity for NMDARE. CSF samples were obtained prior to induction of appropriate immunotherapy. Antibody titers were 1:4 for patient A, 1:10 for patient B, and 1:32 for patient C. Additional CSF samples were obtained from female patients between 29 and 33 years of age with multiple sclerosis (MS), a chronic neuroinflammatory/autoimmune disease (Polman et al., 2011), as well as from neurologically normal volunteers. Patients were enrolled in ongoing prospective observational research studies at Washington University in St. Louis. Neurologically normal volunteers were recruited from the local community, and CSF was obtained following a brief interview (to establish status as controls) and neurological examination. Study protocols were approved by the Washington University School of Medicine Human Research Protections Office. Written informed consent was obtained from patients (or their delegates) and neurologically normal volunteers, permitting collection, storage, and use of CSF in appropriate clinical research studies. CSF was stored at -70° C until use.

In electrophysiological recording and immunohistochemistry experiments, cells were incubated
in 1:12 or 1:24 dilutions of patient CSF, neurologically normal CSF, or artificial CSF (aCSF)
containing in mM: 138 NaCl, 4 KCl, 2 CaCl ₂ , 10 glucose, 10 HEPES 2 CaCl ₂ , 1 MgCl ₂ , and 10
glucose. Glutamate receptor antagonists D-APV (10 $\mu M)$ and NBQX (1 $\mu M)$ were included to
prevent excitotoxicity. Due to limited CSF sample, aliquots were harvested following
experiments and reused up to four times; controls and experimental samples were matched for
number of uses.
N2a Cell Transfection: Murine neuro-2a (N2a; ATCC #CCL-131) cells were cultured in
Dulbecco's Modified Eagle's medium (DMEM) supplemented with 10% (v/v) FBS, 2 mM
glutamine plus 100 U/ml penicillin and 0.1 mg/ml streptomycin in an atmosphere of 5% CO2
and 95% air. Cells were maintained at sub-confluent densities and transiently transfected with
GluN1 (0.34 μg) and GluN2B-SEP (2 μg) subunit DNA. GluN1a in pcDNA3 plasmid was a gift
kindly provided by Dr. Elias Aizenman (Department of Neurobiology, University of Pittsburgh
School of Medicine, Pittsburgh, PA 15261) The pCI-SEP_NR2B subunit was a gift from
Roberto Malinow (Addgene plasmid # 23998)(Kopec et al., 2006). The transfection protocol
consisted of 4 h incubation at 37° C in serum-free medium containing plasmids and
Lipofectamine 2000 reagent (Invitrogen, Carlsbad, CA). Following the incubation, the medium
was exchanged for serum-containing medium including 100 uM ketamine to prevent receptor-
mediated cell death (Boeckman and Aizenman, 1996).
Slice Staining: Rodent brain tissue was fixed, permeabilized and incubated in a 1:20 dilution of

patient CSF, followed by application of anti-human IgG secondary antibody conjugated to Alexa

163 Fluor 555. Images were taken of hippocampus using a 4x objective under epifluorescence 164 illumination. 165 **Electrophysiology:** Whole-cell recording pipettes were pulled from borosilicate glass capillary 166 tubes (World Precision Instruments) and exhibited 2-6 M Ω final open-tip resistances. Unless 167 otherwise stated, neurons were voltage clamped to -70 mV. Electrophysiological extracellular 168 recording solution typically contained: 138 mM NaCl, 4 mM KCl, 2 mM CaCl₂, 10 mM glucose, 169 10 HEPES, 20 μM D-serine, 15 μM gabazine, 1 μM NBQX, and 0.2 μM tetrodotoxin, pH 7.25. Extracellular Mg²⁺ was excluded during electrophysiological evaluation of NMDAR function. 170 171 The whole-cell pipette internal solution contained (in mM): 140 cesium methanesulfonate, 5 172 NaCl, 0.5 CaCl₂, 5 EGTA, and 10 HEPES, pH 7.25. NMDA receptor function was probed by applying 10 µM NMDA for 5 s. 173 174 Evoked EPSCs were obtained from solitary neurons in microcultures with a 1.5 ms 175 depolarization to 0 mV to elicit a breakaway action potential in the cell's axon. For these 176 experiments potassium gluconate replaced cesium methanesulfonate in the pipette solution. 177 Tetrodotoxin was excluded from bath solution, and NBQX was added or excluded as indicated. 178 Access resistance was compensated to 90-95% for evoked autaptic PSC recordings. Some 179 synaptic recordings were obtained in presence of 1 µM NBQX as indicated. 180 Fluorescence imaging and anti-GFP immunostaining: To assess surface receptor presence, 181 we performed acid quenching of superecliptic pHluorin (SEP)-tagged receptor subunits in live 182 cells during time-lapse imaging. Imaging was performed 24-48 h post-transfection. Cells were 183 perfused with electrophysiological extracellular saline containing 2 mM CaCl₂, 1 mM MgCl₂, 10

mM glucose and 10 μM D-APV. 2-[N-morpholino] ethane sulphonic acid (MES) was then

applied by replacing HEPES in the standard saline and setting the pH to 5.5 with HCl. Fluorescence images were acquired with conventional epifluorescence on a Nikon TE2000 inverted microscope and a CCD camera (Roper Scientific) and analyzed using Fiji/ImageJ. For MES-application experiments, fluorescence intensity was measured in a fixed region of interest (ROI) near the membrane over the entirety of perfusion (22.5 seconds). Baseline fluorescence was calculated as the average of pre-MES and post-MES fluorescence to account for time-dependent decreases. This absolute baseline was compared with that at the final image during MES challenge to measure the MES-induced fluorescence change.

For anti-GFP labeling of SEP-tagged surface receptors, transfected N2a cells were incubated in control or patient CSF 24 h post-transfection. After 24 or 48 h of treatment, cultures were fixed for 5 minutes in 4% paraformaldehyde in phosphate buffered saline. Cells were blocked with 10% normal goat serum (NGS) and incubated with rabbit anti-GFP antibody (Life Technologies, catalogue number A6455) for 3 hours at a 1:1000 dilution. Cells were incubated in secondary antibody conjugated to Alexa Fluor 568 for 30 minutes, and mounted onto coverslips for visualization. Cells were imaged on a Nikon TE2000 microscope equipped with a C1 laser scanning confocal module. Single confocal sections through the middle of the cell were analyzed with Fiji/ImageJ. To ensure objectivity, cells were selected for analysis based on SEP fluorescence, without reference to anti-GFP labeling. To assess anti-GFP surface labeling, ROI lines at 30-pixel thickness were drawn through the cell excluding the nucleus. Fluorescence intensity was assessed along the line, using cell exterior as background. Peak fluorescence value within the first 50 pixels was taken as membrane fluorescence, while mean center values (middle 50 points) corresponded to intracellular fluorescence.

207	Experimental Design and Statistical Analysis: For all experiments we employed a 'yoked'
208	design to guard against ancillary causes of NMDAR alteration. Each set of experimental
209	conditions was performed in parallel on sibling cultures. Each replicate experiment contributed a
210	similar number of cells per experimental condition to overall pooled results.
211	
212	Electrophysiology data acquisition and analyses were performed using pCLAMP 10 software
213	(Molecular Devices). Image processing and measurement of fluorescence intensity was acquired
214	in Fiji/ImageJ. Data were processed and plotted using Excel 2011 (Microsoft), and Prism 7
215	(GraphPad). Statistical significance was determined using Student's t tests, one-way ANOVA, or
216	two-way ANOVA as indicated in text and figure legends and as dictated by experimental design.
217	Unless otherwise noted, $post\ hoc$ two-tailed Student's paired or unpaired t tests with Bonferroni
218	correction were used for multiple comparisons of only those comparisons important for testing a
219	priori hypotheses. Significance was defined as a corrected p value equivalent to <0.05.
220	NMDARE-A CSF-induced depression of NMDA current relative to control was demonstrated in
221	the first figure in 2 independent replications. In subsequent figures, this statistical comparison
222	was not repeated to reduce the possibility of type II errors in testing of additional hypotheses.
223	
224	Least-squares minimization algorithms performed in GraphPad Prism or Clampex were used to
225	estimate rate constants using single exponential functions (Emnett et al., 2013).
226	
227	RESULTS
228	Characterization of receptor changes with patient CSF exposure

CSF from NMDARE patient A (32 year-old female, NMDARE-A) yielded staining of rat brain
reminiscent of NMDAR expression (Figure 1A), in contrast with staining using CSF from age-
and sex-matched MS patient A (Figure 1B, MS-A). These results parallel those of previous
studies (Moscato et al., 2014; Dalmau et al., 2017). We next confirmed that 48 h incubation of
hippocampal cultures in NMDARE-A CSF (1:12 dilution in conditioned culture medium)
depressed NMDAR responsiveness compared with a CSF control (Figure 1C-D). Strong
depression of NMDAR current was observed with dilutions as low as 1:24, and with incubations
as brief as 24 h (Figure 1E). By contrast 1:12 dilution of CSF from neurologically normal
volunteers (NN-A, NN-B) or from MS patients (MS-A, MS-B) produced no decrease in
NMDAR function relative to aCSF (48 h incubation, Figure 1F-G). Subsequently, aCSF was
used as a comparator for most experiments.
•
Although surface NMDAR internalization is associated with depression of NMDAR current
Although surface NMDAR internalization is associated with depression of NMDAR current
Although surface NMDAR internalization is associated with depression of NMDAR current induced by purified patient antibodies or by NMDARE patient CSF (Hughes et al., 2010;
Although surface NMDAR internalization is associated with depression of NMDAR current induced by purified patient antibodies or by NMDARE patient CSF (Hughes et al., 2010; Gleichman et al., 2012; Castillo-Gomez et al., 2017), altered function of remaining surface
Although surface NMDAR internalization is associated with depression of NMDAR current induced by purified patient antibodies or by NMDARE patient CSF (Hughes et al., 2010; Gleichman et al., 2012; Castillo-Gomez et al., 2017), altered function of remaining surface NMDARs could influence clinical expression of disease or response to therapy. To investigate
Although surface NMDAR internalization is associated with depression of NMDAR current induced by purified patient antibodies or by NMDARE patient CSF (Hughes et al., 2010; Gleichman et al., 2012; Castillo-Gomez et al., 2017), altered function of remaining surface NMDARs could influence clinical expression of disease or response to therapy. To investigate the function of residual receptors, we examined the effect of patient CSF incubation on NMDAR
Although surface NMDAR internalization is associated with depression of NMDAR current induced by purified patient antibodies or by NMDARE patient CSF (Hughes et al., 2010; Gleichman et al., 2012; Castillo-Gomez et al., 2017), altered function of remaining surface NMDARs could influence clinical expression of disease or response to therapy. To investigate the function of residual receptors, we examined the effect of patient CSF incubation on NMDAR EPSCs, including decay kinetics recorded from solitary cultured neurons. Because of the brief
Although surface NMDAR internalization is associated with depression of NMDAR current induced by purified patient antibodies or by NMDARE patient CSF (Hughes et al., 2010; Gleichman et al., 2012; Castillo-Gomez et al., 2017), altered function of remaining surface NMDARs could influence clinical expression of disease or response to therapy. To investigate the function of residual receptors, we examined the effect of patient CSF incubation on NMDAR EPSCs, including decay kinetics recorded from solitary cultured neurons. Because of the brief presence of glutamate in the synaptic cleft, EPSC decay renders a good estimate for the

251	indistinguishable from control (Figure 2D). Thus, it appears that channel lifetime in response to
252	brief glutamate exposure is not altered by incubation with patient CSF.
253	
254	We also evaluated channel open probability of the total NMDAR population by examining onset
255	and offset kinetics of memantine, an uncompetitive open-channel blocker of NMDARs, during
256	application of exogenous NMDA after 24 h incubation in CSF (Figure 2E-F). In this protocol,
257	decreased P_{open} of channels results in slower onset/offset kinetics for memantine (Emnett et al.,
258	2015). However, antibody-depressed NMDAR function did not mediate a change in kinetics of
259	memantine block/unblock (Figure 2G-H). This finding further suggests that residual surface
260	NMDARs exhibit no substantial change in functionality.
261	
262	Synaptic NMDAR activation is generally considered trophic, while extrasynaptic NMDAR
263	activation is thought to mediate excitotoxic death (Hardingham and Bading, 2010; but see Wroge
264	et al., 2012). Patient-derived NMDAR autoantibodies may differentially affect trafficking of
265	synaptic versus extrasynaptic receptor populations (Mikasova et al., 2012). To determine
266	whether altered balance between synaptic and extrasynaptic receptors might contribute to
267	dysfunction associated with NMDARE, we estimated the contribution of synaptic NMDARs to
268	the total population of NMDARs following incubation with patient CSF. To do so, we used the
269	very slowly dissociating NMDAR open-channel blocker MK-801 to enrich for extrasynaptic
270	receptors (Rosenmund et al., 1995). MK-801 requires channel opening for binding and once
271	bound is nearly irreversible (Huettner and Bean, 1988). Thus, when applied during ongoing
272	synaptic activity, MK-801 preferentially blocks synaptic NMDARs. Upon MK-801 removal,
273	NMDA-elicited current thus arises mainly from the extrasynaptic NMDAR population. Synaptic

activity was elevated during MK-801 application (10 µM, 15 min) with co-incubation in the
$GABA_A$ receptor antagonist bicuculline (15 μM), ensuring that subsequent agonist-elicited
responses would come nearly exclusively from extrasynaptic receptors (Rosenmund et al., 1995;
Hardingham et al., 2002; Wroge et al., 2012). MK-801 treatment was preceded by 24 h
incubation with control aCSF or NMDARE patient A CSF. Following MK-801 removal, our
evaluation of NMDA current revealed no difference in the fraction of pharmacologically isolated
extrasynaptic receptors in NMDARE-A CSF versus control-incubated cells (Figure 3A-D). Thus,
patient CSF exposure does not induce preferential loss of synaptic receptors or extrasynaptic
receptors.
Two major GluN2 subunits, GluN2A and GluN2B, contribute to hippocampal NMDAR
responses. The two classes localize and function differently (Chen et al., 1999; Tovar and
Westbrook, 1999; Izumi et al., 2005). To determine whether one class is preferentially lost with
patient CSF incubation, we used pharmacological isolation with the GluN2B-selective antagonist
ifenprodil (10 uM). NMDARE-A CSF incubation caused no change in the ifenprodil sensitivity
(Figure 3E-H), suggesting that the fractional contribution of GluN2A/GluN2B NMDARs does
not change as a result of patient CSF incubation. In summary, our evidence supports no
preferential loss of NMDARs associated with localization or with particular GluN2 subunit
presence.
Our data suggest that residual NMDAR behavior remains unperturbed, and therefore functionally
intact following exposure to patient CSF. We would expect from previous work that NMDAR
surface expression is diminished to account for the downregulation of NMDAR responses

observed (Hughes et al., 2010; Moscato et al., 2014). To test surface expression in live cells, we
utilized a biological assay with N2a cells transfected with heteromeric NMDA receptors
composed of GluN1 and super ecliptic pHluorin (SEP)-tagged GluN2B subunits. The SEP-tag is
a pH-sensitive GFP variant located at the N-terminus. To test functionality of the SEP-tagged
subunit, we tested N2a cells in whole-cell, patch-clamp studies. GFP-transfected NMDARs
yielded no response to NMDA application while cells transfected with wild type GluN1 and
GluN2B-SEP exhibited robust current in response to NMDA application (219 \pm 23 pA, n=6
control and 6 GluN-transfected cells; $t(10)=8.9$, $p=<1E-4$, Student's unpaired t test).
In live cells fluorescence is quenched by the acidity of intracellular organelles but is brighter in
surface receptors where the tag is exposed to the neutral pH of the extracellular space (Kopec et
al., 2006). Live transfected cells showed robust fluorescence that was quenched by MES, a
membrane impermeant acid (Kopec et al., 2006)(Figure 4A). The baseline fluorescence of SEP-
transfected cells was weaker in transfected cells incubated in NMDARE-A CSF, and MES
quenching was reduced accordingly (Figure 4B). These results implicate a robust loss of surface
receptors with patient CSF treatment.
As an additional check on surface NMDAR presence in GluN1/GluN2B-SEP transfected N2a
cells, we used anti-GFP antibody labeling in fixed, non-permeabilized cells (Figure 4C-J). Cells
transfected with GluN1/GluN2B-SEP exhibited significantly higher membrane-associated anti-
GFP labeling than control cells transfected with cytosolic GFP (Figure 4C-G). In
GluN1/GluN2B-SEP-transfected cells incubated in NMDARE-A and MS-A CSF, anti-GFP

surface labeling was strongly reduced (Figure 4H-J). Thus, both live-cell imaging and

320	immunocytochemistry results support loss of surface receptors following incubation with
321	NMDARE patient CSF.
322	
323	Effects of oxysterol-like PAMs on receptor function following patient CSF exposure.
324	The above results demonstrate that exposure to NMDARE patient CSF mediates broad loss of
325	surface NMDARs, regardless of synaptic localization or subunit composition. It follows,
326	therefore, that treatment with a broad spectrum NMDAR PAM may be a rational approach to
327	enhancing function of remaining surface NMDARs. The major brain cholesterol metabolite 24S-
328	hydroxycholesterol and several synthetic analogues represent a new class of broad-spectrum
329	PAMs (Sun et al., 2015). Subsequently, we evaluated the ability of SGE-301, a previously
330	characterized synthetic oxysterol analogue (Paul et al., 2013), and SGE-550, a similar but
331	previously unreported synthetic PAM, to rescue NMDAR function following exposure to patient
332	CSF.
333	
334	As expected, the acute (30 second) application of either SGE-301 or SGE-550 (2 $\mu M)$
335	potentiated responses to 10 μM NMDA (Figure 5A-C). We explored effects of PAM incubation
336	as an intervention during patient CSF exposure. Following 24 h incubation of cultured
337	hippocampal cells in NMDARE-A CSF, we intervened with a co-application of one of the PAMs
338	for an additional 24 h. Following the full 48 h challenge, we removed the culture medium
339	containing CSF and PAM and placed cells in recording saline free of PAM. Despite the absence
340	of PAM in recording solutions, NMDA responses in both aCSF control conditions and
341	NMDARE-A CSF conditions were significantly augmented (Figure 5D, E). Statistically, there
342	was no interaction between CSF incubation status and PAM treatment status (Figure 5D, E),

indicating that PAMs may not interfere directly with the mechanisms of depressed NMDA current amplitude, including receptor internalization. We followed-up this observation with experimental tests of the mechanism of persistently potentiated NMDA currents following prolonged PAM incubation.

347

348

349

350

351

352

353

354

355

356

357

358

359

360

361

362

363

364

343

344

345

346

We have previously shown that oxysterols are resistant to washout, potentially explaining the persistent effects of PAMs (Paul et al., 2013; Linsenbardt et al., 2014). However, we found no correlation between time of recording following PAM removal and the size of NMDA current in our dataset (not shown). Therefore, we entertained the possibility that oxysterol analogues induce a permanent change in NMDAR function (e.g., by fostering receptor insertion or inhibiting internalization in control and antibody-treated conditions). We used the open-channel blocker memantine to test if persistently increased NMDA current following PAM incubation is associated with increased channel open probability, as expected of PAM action (Emnett et al., 2015). Indeed, cells incubated 24 h with SGE-301 or with SGE-550, but recorded in the absence of PAM, exhibited faster onset and offset memantine kinetics (Figure 6A-D). We further evaluated whether the potentiation of NMDA current results from acute drug presence by briefly incubating cells with the steroid scavenger γ-cyclodextrin (γ-CDX; 500 uM, 2 min)(Akk et al., 2005; Shu et al., 2007; Paul et al., 2013). Although γ-CDX incubation alone appeared to have a mild potentiating effect, the scavenger effectively reversed the persisting PAM potentiation (Figure 6E-G). The rapid reduction produced by the scavenger causes us to conclude that persisting potentiation is most readily explained by lingering compound, likely retained within the membrane and/or sequestered intracellularly.

As a final test of whether PAMs interfere directly with the mechanisms of NMDAR removal, we
returned to N2a cells transfected with SEP tagged GluN subunits to visualize surface receptors.
We imposed the same CSF challenge and PAM intervention as in Figure 4 on cells to assess
surface receptor presence. Cells were incubated for 48 h in NMDARE-A or MS-A CSF with
SGE-301 intervention initiated at 24 h. Following the treatment, cells were fixed and labeled
with anti-GFP antibody (Figure 7A-D). We again observed significant depression of surface
receptor presence in cells treated with NMDARE patient A CSF. SGE-301 did not affect
membrane or intracellular labeling, nor was there a statistically significant interaction between
CSF condition and SGE-301 treatment (Figure 7E-F). This suggests that PAMs do not alter
surface receptor presence, and the observed PAM-associated persisting NMDAR potentiation is
most likely a result of SGE-301's direct interaction with NMDARs.
To extend the proof-of-principle for the PAM therapeutic approach, we examined the effect of
SGE-301 on CSF incubation from two additional NMDARE patients (NMDARE-B, C; Figure
8). Incubation in NMDARE-B and NMDARE-C CSF (23 year and 50 year old females,
respectively, 1.12 dilution for 48 by decreased responses to NADA, and the decreasion was
respectively; 1:12 dilution for 48 h) decreased responses to NMDA, and the depression was
circumvented by incubation in SGE-301, similar to results with NMDARE-A CSF (Figure 8E).
circumvented by incubation in SGE-301, similar to results with NMDARE-A CSF (Figure 8E).
circumvented by incubation in SGE-301, similar to results with NMDARE-A CSF (Figure 8E). These results suggest that the PAM approach may be broadly applicable in patients with
circumvented by incubation in SGE-301, similar to results with NMDARE-A CSF (Figure 8E). These results suggest that the PAM approach may be broadly applicable in patients with

treatments for NMDARE and possibly for other disorders associated with NMDAR

hypofunction, including schizophrenia (Olney and Farber, 1995; Krystal et al., 2002; Lin et al.,
2012; Cioffi, 2013). Using CSF obtained from a patient with a confirmed clinical diagnosis of
NMDARE, we functionally characterized NMDARs in cultured rat hippocampal cells following
incubation with patient CSF, and we quantified characteristics of rescue with two allosteric
modulators of NMDAR function. Persistent effects of compounds restore NMDAR function
through allosteric potentiation of residual NMDARs and suggest that signs and symptoms of
NMDARE may be ameliorated by this therapeutic approach. These cellular studies set a course
for future in vivo tests of the therapeutic approach.
Our study relied primarily on CSF from a single NMDARE patient for which we had sufficient
CSF to permit multiple studies. This patient presented with classic features of NMDARE (see
Methods). Nevertheless, we designed several experiments to test that CSF from NMDARE
patient A possesses features characteristic of NMDARE. Features confirmed in our studies
included CSF labeling (using IgG-specific secondary antibody) of rodent brain tissue in a pattern
expected of NMDAR distribution, functional selective depression of NMDAR current, and loss
of surface NMDARs. We replicated key results in two additional patients with IgG against
NMDARs, confirmed by testing in commercial clinical labs and by our own staining (Figure 8).
In addition, our experiments characterized several new features of NMDAR suppression studied
using NMDARE patient A sample. In contrast with some recent studies (Mikasova et al., 2012),
our results suggest that both synaptic and extrasynaptic receptors are equally targeted for loss.
Although the dimensions and molecular complexity of the synaptic cleft might reduce antibody

access, direct access of various antibodies to the synapse has been demonstrated in numerous

412	previous studies (e.g., Ehlers, 2000; Martens et al., 2008; Mikasova et al., 2012). Thus, it seems
413	likely that both populations of NMDARs are directly targeted by human GluN antibody.
414	Alternatively, interchange between synaptic and extrasynaptic populations (Tovar and
415	Westbrook, 2002) may allow indirect antibody access to synaptic receptors by targeting the
416	extrasynaptic pool. Future time course studies may distinguish these possibilities.
417	
418	Other previous studies have suggested that antibody may alter the function of remaining surface
419	NMDARs. For instance, within minutes following patient CSF exposure, increased channel open
420	duration was detected (Gleichman et al., 2012). Our studies revealed no evidence for increased
421	or decreased open probability of NMDAR channels following prolonged patient CSF exposure,
422	using an open-channel blocker as a probe of channel open probability in whole-cell recordings
423	(Huettner and Bean, 1988). Discrepancies with previous work may reflect differences in the time
424	at which measurements were made or heterogeneity in the clinical population. These hypotheses
425	can be tested as additional patient material becomes available.
426	
427	Taken together, our findings suggest that treatment with PAMs may represent a potential strategy
428	to rescue NMDAR hypofunction, with no detectable direct effect on the mechanisms of NMDAR
429	internalization that characterize the cellular pathophysiology. A more direct approach to maintain
430	or restore NMDAR function would be to target the cell biological mechanisms responsible for
431	receptor endocytosis and insertion; however, at this time, pharmacological interventions
432	targeting these mechanisms are not practical. Therefore, we made use of emerging understanding
433	of a class of positive regulators of NMDAR function that has resulted from study of the
434	endogenous cholesterol metabolite. 24S-hydroxycholesterol (Sun et al., 2015).

SGE-301 and SGE-550 represent synthetic analogues of 24S-hydroxycholesterol with selective
NMDAR effects in the sub-to-low micromolar concentration range (Paul et al., 2013;
Linsenbardt et al., 2014). These compounds appear to bind to a site independent of other known
allosteric modulators of NMDAR function (Paul et al., 2013; Wilding et al., 2016) and increase
channel open probability. Results with chimeric GluN –GluK subunits suggest that GluN
transmembrane domains are critical for oxysterol modulation (Wilding et al., 2016). A
transmembrane interaction site would be consistent with the lipophilic nature of these modulators
and with their sensitivity to cyclodextrin extraction (Shu et al., 2007). Interaction of oxysterols
with NMDARs results in a slight reduction in the EC50 of agonists and increased agonist
efficacy (Linsenbardt et al., 2014). Here we show that several dilutions of NMDARE patient
CSF result in similar presumed steady-state NMDAR reductions (Figure 1). The mechanisms
responsible for a fixed steady-state level of functional receptors despite varied antibody
concentration are unclear. We found that low micromolar concentrations of allosteric modulators
restored the activity of NMDARs from this steady-state to near or above baseline levels (Figures
5,6,8).
A puzzling observation initially was that potentiated NMDAR function persisted beyond the
period of direct exposure to compounds in all cells incubated in SGE-301 or SGE-550. We found
that the enhanced function was associated with increased channel open probability, was sensitive
to a scavenger of lipophilic compounds, and was not associated with increased surface
NMDARs. Thus, we attribute the persistence to the strong lipophilicity of the modulators. We
have previously shown evidence of modulator persistence for at least tens of seconds (Paul et al.

459

460

461

462

463

464

465

466

467

468

469

470

471

472

473

474

475

476

477

478

479

480

2013). The present studies confirm that some oxysterol-like compounds can persist for many minutes beyond removal, presumably by adhering to cells or accumulating intracellularly, potentiating NMDAR responses despite constant local perfusion with compound-free saline. This persistence of drug binding becomes relevant when assessing the rapeutic viability, recognizing that strong lipophilicity may be advantageous to dosing schedules. However, drug exposure in a clinical setting would presumably last beyond the 24 h incubation period used herein and could result in other changes not appreciated here. Additional in vivo studies are required to clarify the time-dependent effects, and effect of dosing regimen on NMDAR function. Our work focused on the restorative actions of NMDAR modulators following exposure to CSF from NMDARE patients. The idea that NMDAR hypofunction accounts for the broad spectrum of clinical symptomatology described in NMDARE is supported by two primary lines of evidence. First, pharmacologically-induced NMDAR hypofunction produces psychotomimetic symptoms, not unlike those observed in NMDARE. Second, intrathecal injection of recombinant antibodies can recapitulate key aspects of the disorder in rodents (Malviya et al., 2017). We acknowledge, however, that additional pathogenic processes downstream of NMDAR internalization, or other CSF constituents (e.g., other disease-associated antibodies or inflammatory mediators; Kreye et al., 2016) may affect neuronal function and contribute to

suppression of NMDAR function (e.g., the stronger suppression observed in NMDARE patient

A vs. patients B and C). Others may be unrelated to NMDAR function ant thus not modulated

by NMDAR PAMs. Furthermore, sample quantities limited culture studies to relatively brief

symptomatology. Some of these may account for apparent differences in the degree of

periods of exposure, unlike the clinical situation where antibody is constantly renewed, resulting
in prolonged exposure. For these reasons, it will be important to adopt robust animal models and
follow-up the cellular level studies herein with circuit-level and in vivo tests of the therapeutic
potential of NMDAR PAMs in NMDARE (Planaguma et al., 2015; Malviya et al., 2017).
Our work shows that indiscriminate loss of NMDARs occurs following exposure to NMDARE
patient CSF, and suggests that PAMs may be developed as a potential therapeutic strategy.
Restoration of NMDAR function was achieved with application of oxysterol analogues, which
are potent, selective, but broad spectrum PAMs of NMDAR function. The restorative effects
were fully accounted for by the acute pharmacological effects of the compounds.

493	
494	REFERENCES
495	Akk G, Shu HJ, Wang C, Steinbach JH, Zorumski CF, Covey DF, Mennerick S (2005)
496	Neurosteroid access to the GABA _A receptor. J Neurosci 25:11605-11613.
497	Anticevic A, Gancsos M, Murray JD, Repovs G, Driesen NR, Ennis DJ, Niciu MJ, Morgan PT,
498	Surti TS, Bloch MH, Ramani R, Smith MA, Wang XJ, Krystal JH, Corlett PR (2012)
499	NMDA receptor function in large-scale anticorrelated neural systems with implications
500	for cognition and schizophrenia. Proc Natl Acad Sci USA 109:16720-16725.
501	Boeckman FA, Aizenman E (1996) Pharmacological properties of acquired excitotoxicity in
502	Chinese hamster ovary cells transfected with N-methyl-D-aspartate receptor subunits. J
503	Pharmacol Exp Ther 279:515-523.
504	Castillo-Gomez E, Oliveira B, Tapken D, Bertrand S, Klein-Schmidt C, Pan H, Zafeiriou P,
505	Steiner J, Jurek B, Trippe R, Pruss H, Zimmermann WH, Bertrand D, Ehrenreich H,
506	Hollmann M (2017) All naturally occurring autoantibodies against the NMDA receptor
507	subunit NR1 have pathogenic potential irrespective of epitope and immunoglobulin class.
508	Mol Psychiatry In Press.
509	Chen N, Luo T, Raymond LA (1999) Subtype-dependence of NMDA receptor channel open
510	probability. J Neurosci 19:6844-6854.
511	Cioffi CL (2013) Modulation of NMDA receptor function as a treatment for schizophrenia.
512	Bioorg Med Chem Lett 23:5034-5044.
513	Dalmau J, Geis C, Graus F (2017) Autoantibodies to synaptic receptors and neuronal cell surface
514	proteins in autoimmune diseases of the central nervous system. PhysiolRev 97:839-887.
515	Dubey D, Pittock SJ, Kelly CR, McKeon A, Lopez-Chiriboga AS, Lennon V, Gadoth A, Smith
516	CY, Bryant SC, Klein CJ, Aksamit AJ, Toledano M, Boeve BF, Tilemma JM, Flanagan

517	EP (2018) Autoimmune encephalitis epidemiology and a comparison to infectious
518	encephalitis. Ann Neurol.
519	Ehlers MD (2000) Reinsertion or Degradation of AMPA Receptors Determined by Activity-
520	Dependent Endocytic Sorting. Neuron 28:511-525.
521	Emnett CM, Eisenman LN, Mohan J, Taylor AA, Doherty JJ, Paul SM, Zorumski CF,
522	Mennerick S (2015) Interaction between positive allosteric modulators and trapping
523	blockers of the NMDA receptor channel. Br J Pharmacol 172:1333-1347.
524	Finke C, Kopp UA, Pajkert A, Behrens JR, Leypoldt F, Wuerfel JT, Ploner CJ, Pruss H, Paul F
525	(2016) Structural hippocampal damage following anti-N-Methyl-D-Aspartate receptor
526	encephalitis. Biol Psychiatry 79:727-734.
527	Fischer CE, Golas AC, Schweizer TA, Munoz DG, Ismail Z, Qian W, Tang-Wai DF, Rotstein
528	DL, Day GS (2016) Anti N-methyl-D-aspartate receptor encephalitis: a game-changer?
529	Expert Rev Neurother 16:849-859.
530	Gabilondo I, Saiz A, Galan L, Gonzalez V, Jadraque R, Sabater L, Sans A, Sempere A, Vela A,
531	Villalobos F, Vinals M, Villoslada P, Graus F (2011) Analysis of relapses in anti-
532	NMDAR encephalitis. Neurology 77:996-999.
533	Gable MS, Sheriff H, Dalmau J, Tilley DH, Glaser CA (2012) The frequency of autoimmune N-
534	methyl-D-aspartate receptor encephalitis surpasses that of individual viral etiologies in
535	young individuals enrolled in the California Encephalitis Project. Clin Infect Dis 54:899-
536	904.
537	Gleichman AJ, Spruce LA, Dalmau J, Seeholzer SH, Lynch DR (2012) Anti-NMDA receptor
538	encephalitis antibody binding is dependent on amino acid identity of a small region
539	within the GluN1 amino terminal domain. J Neurosci 32:11082-11094.

540	Hardingham GE, Bading H (2010) Synaptic versus extrasynaptic NMDA receptor signalling:
541	implications for neurodegenerative disorders. Nat Rev Neurosci 11:682-696.
542	Hardingham GE, Fukunaga Y, Bading H (2002) Extrasynaptic NMDARs oppose synaptic
543	NMDARs by triggering CREB shut-off and cell death pathways. Nat Neurosci 5:405-
544	414.
545	Huettner JE, Bean BP (1988) Block of N-methyl-D-aspartate- activated current by the
546	anticonvulsant MK-801: selective binding to open channels. Proc Natl Acad Sci USA
547	85:1307-1311.
548	Hughes EG, Peng X, Gleichman AJ, Lai M, Zhou L, Tsou R, Parsons TD, Lynch DR, Dalmau J,
549	Balice-Gordon RJ (2010) Cellular and synaptic mechanisms of anti-NMDA receptor
550	encephalitis. J Neurosci 30:5866-5875.
551	Izumi Y, Nagashima K, Murayama K, Zorumski CF (2005) Acute effects of ethanol on
552	hippocampal long-term potentiation and long-term depression are mediated by different
553	mechanisms. Neuroscience 136:509-517.
554	Kopec CD, Li B, Wei W, Boehm J, Malinow R (2006) Glutamate receptor exocytosis and spine
555	enlargement during chemically induced long-term potentiation. J Neurosci 26:2000-2009.
556	Kreye J et al. (2016) Human cerebrospinal fluid monoclonal N-methyl-D-aspartate receptor
557	autoantibodies are sufficient for encephalitis pathogenesis. Brain 139:2641-2652.
558	Krystal JH, Anand A, Moghaddam B (2002) Effects of NMDA receptor antagonists:
559	implications for the pathophysiology of schizophrenia. Arch Gen Psychiatry 59:663-664.
560	Lester RA, Clements JD, Westbrook GL, Jahr CE (1990) Channel kinetics determine the time
561	course of NMDA receptor- mediated synaptic currents. Nature 346:565-567.

562	Lin CH, Lane HY, Tsai GE (2012) Glutamate signaling in the pathophysiology and therapy of
563	schizophrenia. Pharmacol Biochem Behav 100:665-677.
564	Linsenbardt AJ, Taylor A, Emnett CM, Doherty JJ, Krishnan K, Covey DF, Paul SM, Zorumski
565	CF, Mennerick S (2014) Different oxysterols have opposing actions at N-methyl-D-
566	aspartate receptors. Neuropharmacology 85:232-242.
567	Malviya M et al. (2017) NMDAR encephalitis: passive transfer from man to mouse by a
568	recombinant antibody. Annals of Clinical and Translational Neurology:n/a-n/a.
569	Martens H, Weston MC, Boulland JL, Gronborg M, Grosche J, Kacza J, Hoffmann A, Matteoli
570	M, Takamori S, Harkany T, Chaudhry FA, Rosenmund C, Erck C, Jahn R, Hartig W
571	(2008) Unique luminal localization of VGAT-C terminus allows for selective labeling of
572	active cortical GABAergic synapses. J Neurosci 28:13125-13131.
573	Mikasova L, De Rossi P, Bouchet D, Georges F, Rogemond V, Didelot A, Meissirel C, Honnorat
574	J, Groc L (2012) Disrupted surface cross-talk between NMDA and Ephrin-B2 receptors
575	in anti-NMDA encephalitis. Brain 135:1606-1621.
576	Moscato EH, Peng X, Jain A, Parsons TD, Dalmau J, Balice-Gordon RJ (2014) Acute
577	mechanisms underlying antibody effects in anti-N-methyl-D-aspartate receptor
578	encephalitis. Ann Neurol 76:108-119.
579	Olney JW, Farber NB (1995) Glutamate receptor dysfunction and schizophrenia. Arch Gen
580	Psychiatry 52:998-1007.
581	Panzer JA, Lynch DR (2013) Neuroimmunology: Treatment of anti-NMDA receptor
582	encephalitis-time to be bold? Nat Rev Neurol 9:187-189.
583	Paul SM, Doherty JJ, Robichaud AJ, Belfort GM, Chow BY, Hammond RS, Crawford DC,
584	Linsenbardt AJ, Shu HJ, Izumi Y, Mennerick SJ, Zorumski CF (2013) The major brain

585	cholesterol metabolite 24(S)-hydroxycholesterol is a potent allosteric modulator of N-
586	methyl-D-aspartate receptors. J Neurosci 33:17290-17300.
587	Planaguma J, Leypoldt F, Mannara F, Gutierrez-Cuesta J, Martin-Garcia E, Aguilar E, Titulaer
588	MJ, Petit-Pedrol M, Jain A, Balice-Gordon R, Lakadamyali M, Graus F, Maldonado R,
589	Dalmau J (2015) Human N-methyl D-aspartate receptor antibodies alter memory and
590	behaviour in mice. Brain 138:94-109.
591	Polman CH, Reingold SC, Banwell B, Clanet M, Cohen JA, Filippi M, Fujihara K, Havrdova E,
592	Hutchinson M, Kappos L, Lublin FD, Montalban X, O'Connor P, Sandberg-Wollheim M
593	Thompson AJ, Waubant E, Weinshenker B, Wolinsky JS (2011) Diagnostic criteria for
594	multiple sclerosis: 2010 revisions to the McDonald criteria. Ann Neurol 69:292-302.
595	Rosenmund C, Feltz A, Westbrook G (1995) Synaptic NMDA receptor channels have a low
596	open probability. J Neurosci 15:2788-2795.
597	Shu HJ, Zeng CM, Wang C, Covey DF, Zorumski CF, Mennerick S (2007) Cyclodextrins
598	sequester neuroactive steroids and differentiate mechanisms that rate limit steroid actions
599	Br J Pharmacol 150:164-175.
600	Sun MY, Linsenbardt AJ, Emnett CM, Eisenman LN, Izumi Y, Zorumski CF, Mennerick S
601	(2015) 24(S)-Hydroxycholesterol as a modulator of neuronal signaling and survival.
602	Neuroscientist.
603	Titulaer MJ, McCracken L, Gabilondo I, Armangue T, Glaser C, Iizuka T, Honig LS, Benseler
604	SM, Kawachi I, Martinez-Hernandez E, Aguilar E, Gresa-Arribas N, Ryan-Florance N,
605	Torrents A, Saiz A, Rosenfeld MR, Balice-Gordon R, Graus F, Dalmau J (2013)
606	Treatment and prognostic factors for long-term outcome in patients with anti-NMDA
607	receptor encephalitis: an observational cohort study. Lancet Neurol 12:157-165.

808	Tovar KR, Westbrook GL (1999) The incorporation of NMDA receptors with a distinct subunit
609	composition at nascent hippocampal synapses in vitro. J Neurosci 19:4180-4188.
610	Tovar KR, Westbrook GL (2002) Mobile NMDA receptors at hippocampal synapses. Neuron
611	34:255-264.
612	Wilding TJ, Lopez MN, Huettner JE (2016) Chimeric glutamate receptor subunits reveal the
613	transmembrane domain is sufficient for NMDA receptor pore properties but some
614	positive allosteric modulators require additional domains. J Neurosci 36:8815-8825.
615	Wroge CM, Hogins J, Eisenman L, Mennerick S (2012) Synaptic NMDA receptors mediate
616	hypoxic excitotoxic death. J Neurosci 32:6732-6742.
617	Zorumski CF, Izumi Y, Mennerick S (2016) Ketamine: NMDA Receptors and Beyond. J
618	Neurosci 36:11158-11164.
619	
520	

621	FIGURES AND LEGENDS
622	Figure 1. Depression of NMDA current in hippocampal neurons following patient CSF
623	incubation. A. NMDARE-A CSF (1:20 dilution) labels mouse hippocampus in a pattern typical
624	of NMDAR distribution. Human antibody binding to the tissue section was visualized with anti-
625	human secondary antibody conjugated to Alexa Fluor 555. B. CSF from an age- and sex-
626	matched MS patient (1:20 dilution), failed to exhibit an NMDAR-like pattern of labeling. C.
627	NMDA (10 μ M)-elicited current from a hippocampal neuron following 48 h incubation with
628	either aCSF (1:12, black trace) or NMDARE-A CSF (1:12, red trace). D. Summary of NMDA
629	current density from cells treated as in C; (t(46)=6.951, *p=1.08E-8) (n=21 for control and 27
630	for NMDARE-A). E. Comparison of effects of two dilutions of NMDARE-A CSF: 24 h in either
631	1:12 dilution (n =10) or 1:24 dilution (n =10) in sibling cultures. A one-way ANOVA showed a
632	significant NMDARE-A CSF-mediated current depression (F(2,27)=14.1, *p= 6.6E-5). Asterisks
633	denote p <0.05 versus aCSF, determined with Student's unpaired t test, Bonferroni corrected for
634	multiple comparisons. F. Representative traces from an experiment examining NMDA (10 $\mu\text{M})\text{-}$
635	elicited current from a hippocampal neuron following 48 h incubation of hippocampal cultures in
636	aCSF (1:12 black trace, $n=15$) or CSF from MS-A (1:12, gray trace, $n=10$). G. Control CSF
637	from age- and sex-matched MS patients (MS-A, MS-B) and neurologically normal controls (NN-
638	A, NN-B). There was no significant difference between any treated group and control; $p>0.05$
639	uncorrected t tests.
640	

Figure 2. Lack of change in key functional properties of residual NMDARs. **A** and **B**. Evoked autaptic EPSCs from a hippocampal neuron incubated with aCSF (A) or NMDARE-A CSF (B). Dual-component AMPAR and NMDAR EPSCs (light traces) and pharmacologically isolated

644	NMDAR EPSCs (dark traces) are shown. C. Summary of ratio of NMDAR to AMPAR peak
645	EPSC; (t(14)=4.2, *p=1E-9, Student's unpaired t test. D. Summary of weighted time constant
646	values (τ_{w}) obtained from a bi-exponential fit to the decay phase of the NMDAR EPSCs;
647	(t(14)=1.15, p=0.27, Student's unpaired t test). E and F . The rapid onset/offset open-channel
648	blocker memantine was used to probe changes in NMDAR channel open probability. G . and H .
649	Summary of the memantine onset and offset kinetics (obtained from exponential fits) revealed no
650	change following NMDARE-A CSF-mediated depression; (G: t(7)=1.15, p=0.29;
651	H:t(13)=1.33,p=0.21 respectively, Student's unpaired t tests).
652	
653	Figure 3. No evidence of selective effect of NMDARE-A CSF on proportion of extrasynaptic
654	NMDARs or on the proportion of GluN2B-containing receptors. A and B. NMDA-elicited
655	current from neurons without (black) and with (blue) preceding MK-801 challenge to block
656	synaptic receptors. C. Summary of raw NMDA current density of respective ±MK-801
657	conditions. Analysis of raw current density revealed no interaction between condition
658	(aCSF/NMDARE-A CSF) and treatment (\pm MK-801; F (1, 52) = 0.36, two-way ANOVA,
659	p>0.55). D. Summary of MK-801 effect, normalized to the mean current density of the
660	respective -MK-801 condition (right). Analysis of normalized data also revealed no change in the
661	proportion of MK-801 insensitive current following NMDARE-A CSF incubation; (t(42)=0.93,
662	$p>0.36$, Student's unpaired t test). E and F . Representative examples of ifenprodil (10 μ M)
663	sensitivity of NMDA-elicited current. G. Summary of raw NMDA current density in baseline
664	and ifenprodil conditions. There was no statistical interaction between condition
665	(aCSF/NMDARE-A CSF) and treatment (\pm ifenprodil; F (1, 48) = 0.7209, p=0.4, two-way
666	ANOVA, $p>0.05$). H. Summary of ifenprodil effect, normalized to the respective baseline

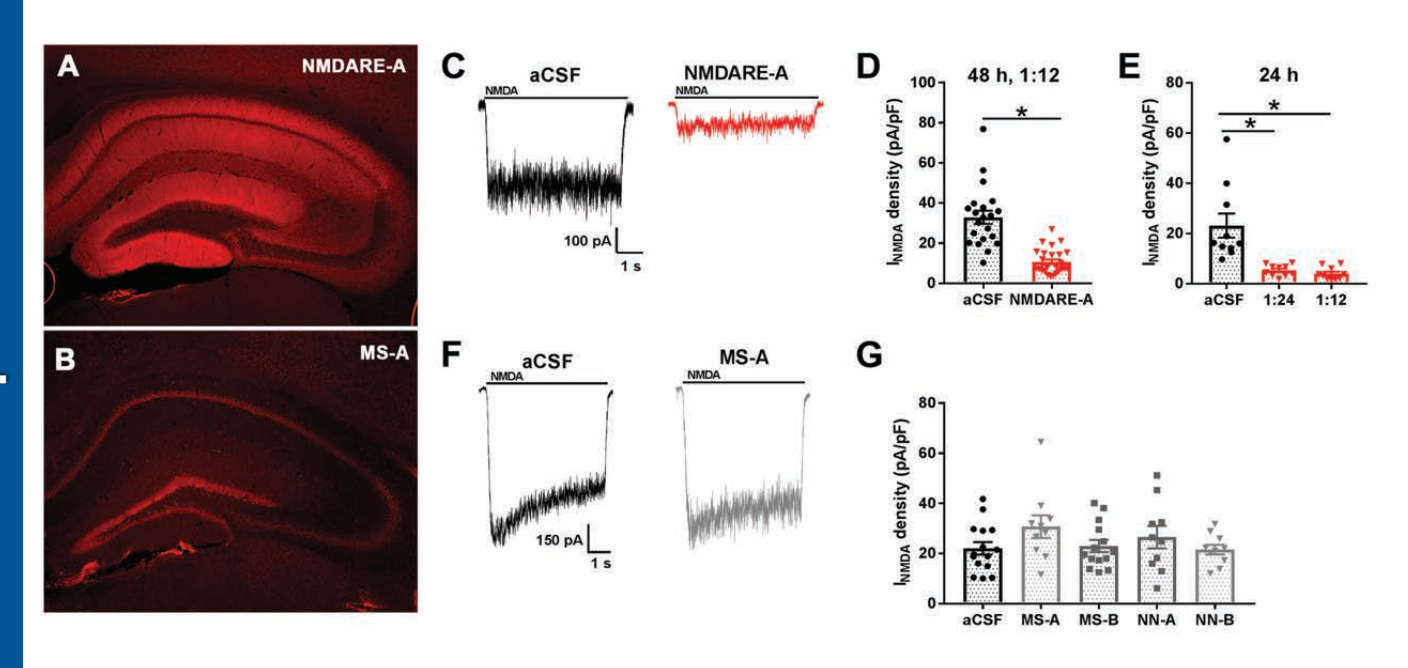
667 current density. Analysis of normalized data also revealed no change in the proportion of 668 ifenprodil-sensitive current following NMDARE-A CSF incubation; (t(24)=0.74, p=0.47, 669 Student's unpaired *t* test). 670 671 Figure 4: NMDARE-A CSF depresses surface NMDAR presence. A. Fluorescence quenching 672 associated with surface NMDARs. N2a cells transfected with GluN1/GluN2B-SEP (super-673 ecliptic pHluorin) were used to visualize NMDARs on the plasma membrane. Transient wash 674 with cell-impermeant MES quenched fluorescence in control cells. Scale bar 10 μm. **B.** 675 Comparison of MES quenching in control cells and cells incubated in NMDARE-A CSF for 24 676 hours. The absolute MES-induced change in fluorescence between cells treated with MS-A CSF 677 (n = 21 cells) vs. NMDARE-A CSF (n = 21 cells from 4 independent replicates) was 678 significantly different (t(40)=2.4, *p=0.02, Student's unpaired t test). **C-G.** Surface receptors detected using anti-GFP labeling of fixed, non-permeabilized transfected N2a cells. Cells were 679 680 transfected with GluN1/GluN2B-SEP subunits or with cytosolic GFP as a control. Analysis lines 681 (yellow) through labeled cells in various conditions yielded evidence for surface receptors (red anti-GFP antibody labeling) in GluN2B-SEP-transfected cells labeled with primary antibody but 682 683 not in other control conditions (Pri = primary antibody incubated). Significant membrane 684 labeling was detected in SEP-transfected cells labeled with primary antibody, compared with 685 other indicated conditions (Bonferroni corrected Student's unpaired t test, *p<0.05). For G686 numbers on bars indicate pooled cell number from 4 experiments. Scale bar 10 µm. H-J. Anti-687 GFP used to label surface NMDARs in transfected N2a cells incubated for 24 h in MS-A CSF or 688 in NMDARE-A CSF, prior to fixation. NMDARE-A CSF reduced anti-GFP membrane labeling

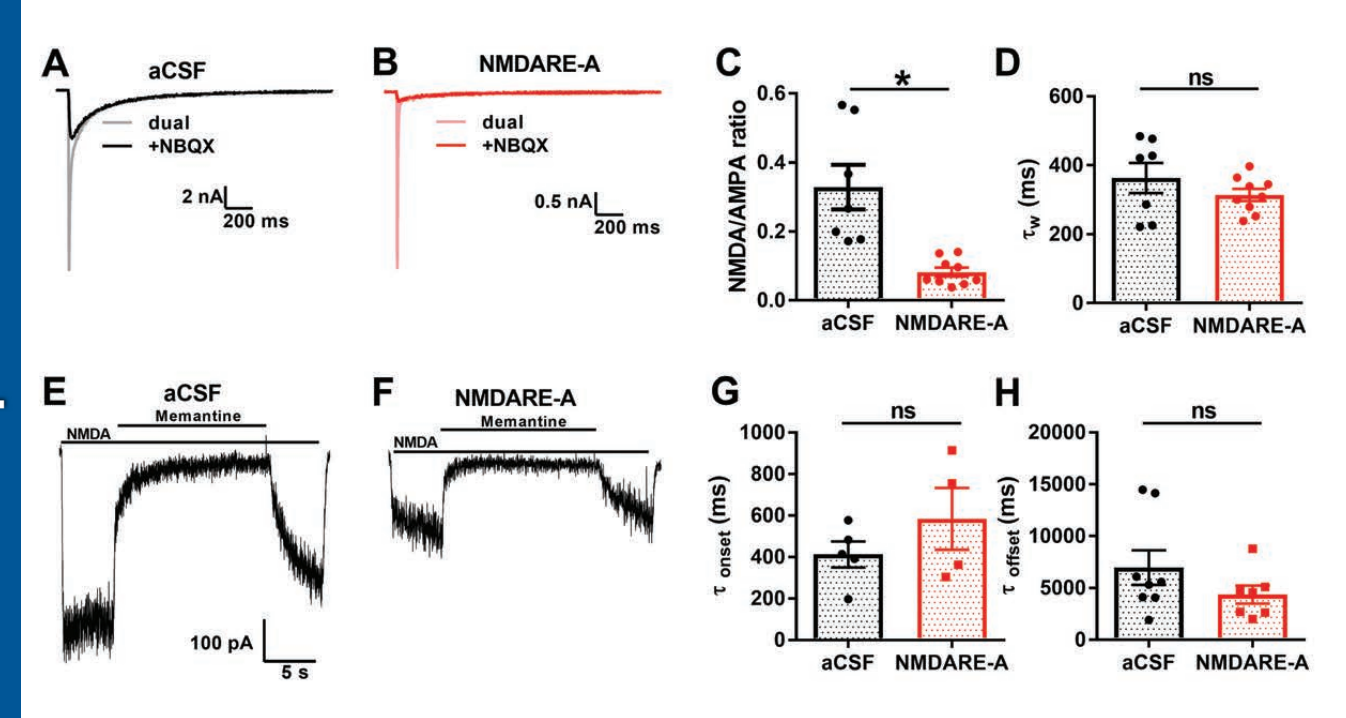
(Bonferroni corrected Student's unpaired t test, *p<0.05).

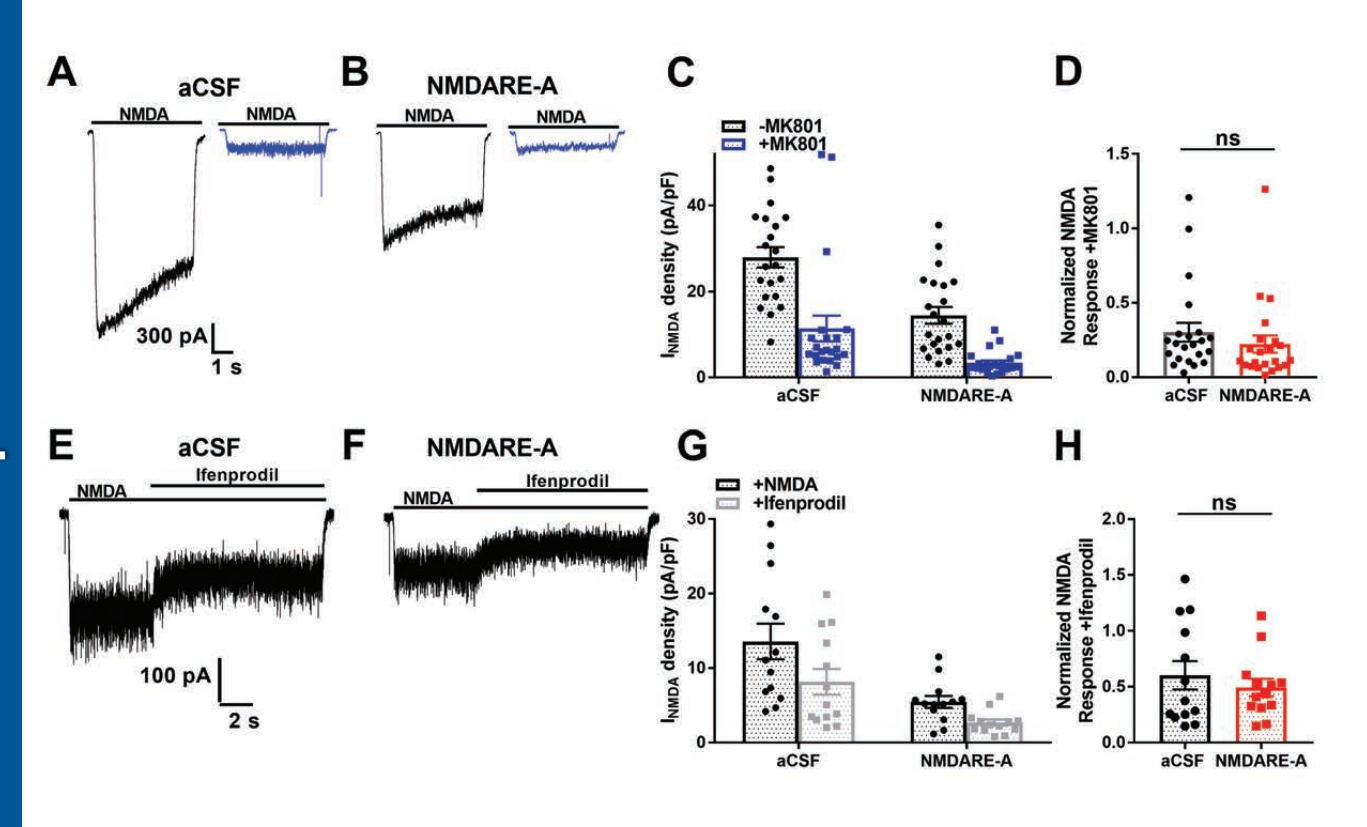
Figure 5. Intervention by oxysterol-mimetic PAMs. A and B. Acute potentiation of NMDA-
elicited current by SGE-301 (2 $\mu M,A)$ and by SGE-550 (2 $\mu M,B).$ PAM was pre-applied for 30
s before co-application with NMDA (colored traces). C. Normalized current showed significant
potentiation by both SGE-301(t(27)=4.3, *p=2E-4) and SGE-550 (t(63)=4.3, *p <1E-4, paired
Student's t tests). D and E . Summary of NMDA-elicited current density recorded following 48 h
of incubation with either aCSF or NMDARE-A CSF, with or without SGE-301 (D) or SGE-550
(E) treatment at 24 h. Two-way ANOVA with Bonferroni corrected post hoc t tests indicated
significant potentiation in aCSF and CSF conditions for both SGE-301 and SGE-550 (* p <0.05).
There was no statistical interaction between CSF condition and either SGE-301 (D: F(1, 56) =
0.5132, p=0.48) or SGE-550 (E: F(1, 125) = 2.121, p=0.15) treatment. Currents were obtained in
recording saline, following removal of CSF and PAM in the culture medium.
Figure 6. Tests of residual PAM activity to explain persisting potentiation. A and B. Memantine
Figure 6. Tests of residual PAM activity to explain persisting potentiation. A and B. Memantine test of NMDAR channel open probability following 24 h aCSF incubation (A) or incubation with
test of NMDAR channel open probability following 24 h aCSF incubation (A) or incubation with
test of NMDAR channel open probability following 24 h aCSF incubation (A) or incubation with SGE-301 (B). C and D . Summary of memantine onset and offset time constant values, obtained
test of NMDAR channel open probability following 24 h aCSF incubation (A) or incubation with SGE-301 (B). C and D . Summary of memantine onset and offset time constant values, obtained from exponential fits; C onset: t(13)=3.1, *p=1.6E-3; C offset t(25)=3.9, *p=6E-4; D
test of NMDAR channel open probability following 24 h aCSF incubation (A) or incubation with SGE-301 (B). C and D . Summary of memantine onset and offset time constant values, obtained from exponential fits; C onset: t(13)=3.1, *p=1.6E-3; C offset t(25)=3.9, *p=6E-4; D onset:t(12)=2.8, *p=1.6E-2; D offset: t(12)=3.9, *p=2E-3, Student's unpaired <i>t</i> tests. E. Sample
test of NMDAR channel open probability following 24 h aCSF incubation (A) or incubation with SGE-301 (B). C and D . Summary of memantine onset and offset time constant values, obtained from exponential fits; C onset: $t(13)=3.1$, *p=1.6E-3; C offset $t(25)=3.9$, *p=6E-4; D onset: $t(12)=2.8$, *p=1.6E-2; D offset: $t(12)=3.9$, *p=2E-3, Student's unpaired t tests. E. Sample traces from cultures incubated under control or in SGE-301 (2 μ M) for 24 h then rinsed with
test of NMDAR channel open probability following 24 h aCSF incubation (A) or incubation with SGE-301 (B). C and D . Summary of memantine onset and offset time constant values, obtained from exponential fits; C onset: $t(13)=3.1$, *p=1.6E-3; C offset $t(25)=3.9$, *p=6E-4; D onset: $t(12)=2.8$, *p=1.6E-2; D offset: $t(12)=3.9$, *p=2E-3, Student's unpaired t tests. E. Sample traces from cultures incubated under control or in SGE-301 (2 μ M) for 24 h then rinsed with saline or γ -CDX (500 μ M) for 2 min before recording. F and G . Summary of effect of brief CDX
test of NMDAR channel open probability following 24 h aCSF incubation (A) or incubation with SGE-301 (B). C and D . Summary of memantine onset and offset time constant values, obtained from exponential fits; C onset: $t(13)=3.1$, *p=1.6E-3; C offset $t(25)=3.9$, *p=6E-4; D onset: $t(12)=2.8$, *p=1.6E-2; D offset: $t(12)=3.9$, *p=2E-3, Student's unpaired t tests. E. Sample traces from cultures incubated under control or in SGE-301 (2 μ M) for 24 h then rinsed with saline or γ -CDX (500 μ M) for 2 min before recording. F and G . Summary of effect of brief CDX incubation on residual SGE-301 (F) and SGE-550 (G). A two-way ANOVA showed a significant

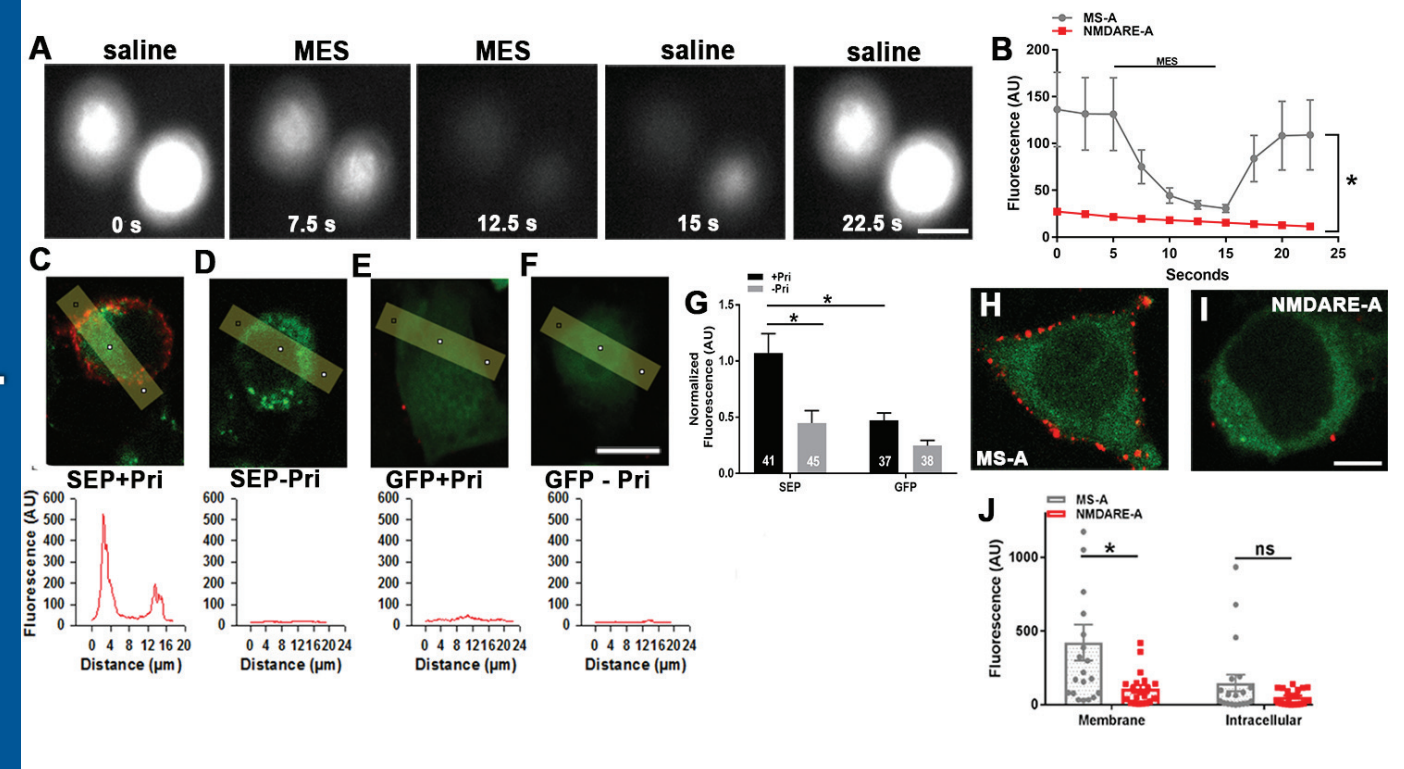
713	Figure 7: No effect of SGE-301 intervention on surface NMDAR presence. A-D. Examples of
714	GluN1/GluN2B-SEP-transfected N2a cells incubated under the indicated conditions. Cells were
715	incubated in CSF for 48 h and incubation with SGE-301 commenced 24 h following CSF
716	initiation. Anti-GFP labeling (red) in non-permeabilized cells was used to quantify surface
717	NMDARs. Green labeling represents SEP fluorescence following fixation. E and F . Two-way
718	ANOVA with Bonferroni corrected post hoc t tests indicated significant depression of surface
719	labeling after incubation in NMDARE-A CSF (E: t(38)=3.0, *p=4.8E-3). There was no statistical
720	interaction between SGE-301 and CSF condition (E: F(1,76)=0.75, p=0.39). SGE-301 did not
721	affect membrane (E) or intracellular anti-GFP labeling (F) in post hoc testing (p $>$ 0.05,
722	Bonferroni corrected <i>t</i> tests).
723	
724	Figure 8. Effect of SGE-301 intervention on depression induced by CSF from a second
725	NMDARE patient. A-C. Staining performed as in Figure 1A,B for 2 additional patient samples
726	and a control sample. D. Sample traces representative of the indicated conditions. NMDARE-B
727	CSF was incubated for 48 h at 1:12 dilution. Intervention with 2 μ M SGE-301 commenced at 24
728	h. E. Summary of effect of incubation with NMDARE-B CSF and intervention with SGE-301. A
729	two-way ANOVA showed a significant main effect of SGE-301 (F(1,59)=11.9, *p=1.0E-3)
730	(asterisk associated with legend) but no interaction with CSF incubation condition
731	(F(1,59)=1.02, p=0.32). Post hoc testing revealed significant depression of NMDA-mediated
732	current induced by NMDARE-B CSF compared with the aCSF condition (t(29)=2.38, *p=.02,
733	Student's unpaired t test). F. Same protocol and statistics as depicted in D and E applied to
734	patient NMDAR-C. A two-way ANOVA showed a significant main effect of SGE-
735	301(F(1,48)=9.71, *p=3.1E-3) but no interaction with CSF incubation condition (F(1,48)=0.26,

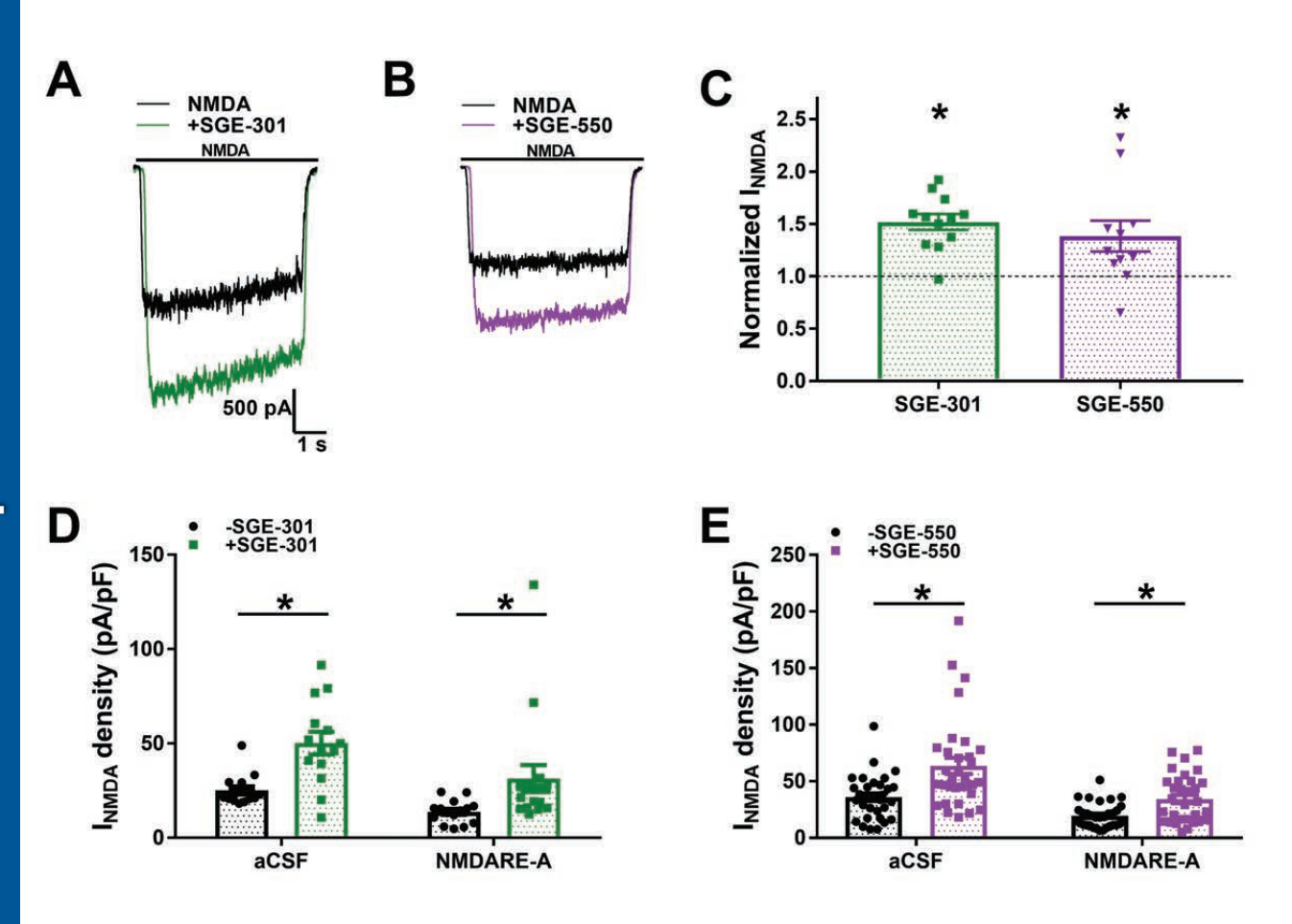
736	p=0.61). Post hoc testing revealed significant depression of NMDA-mediated current induced by
737	NMDARE-B CSF compared with the aCSF condition (t(24)=2.99, *p=6.4E-3, Student's
738	unpaired t test). One data point in the aCSF+SGE-301 condition >120 pA/pF is not shown on the
739	graph for clarity but was used in statistics.
740	
741	

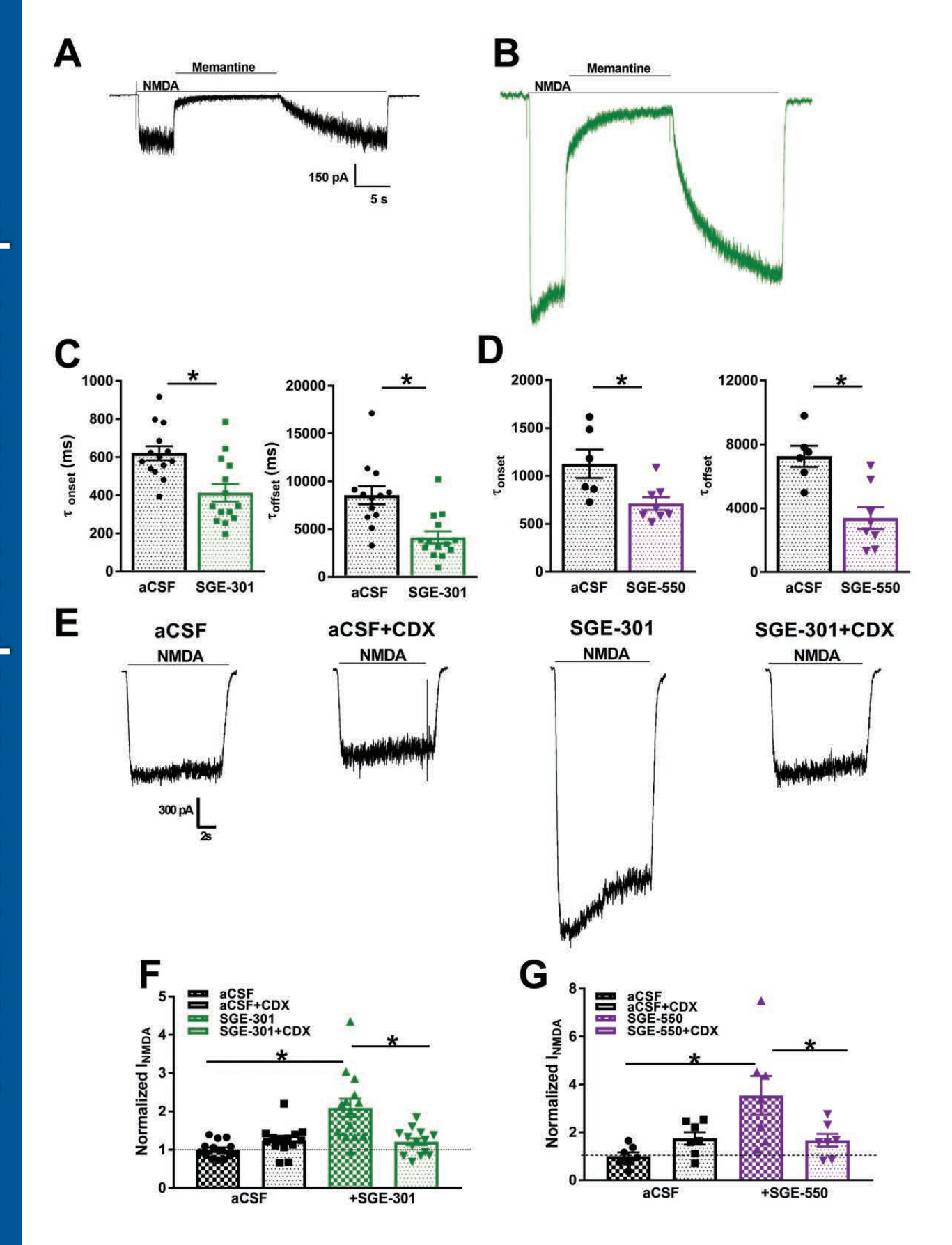


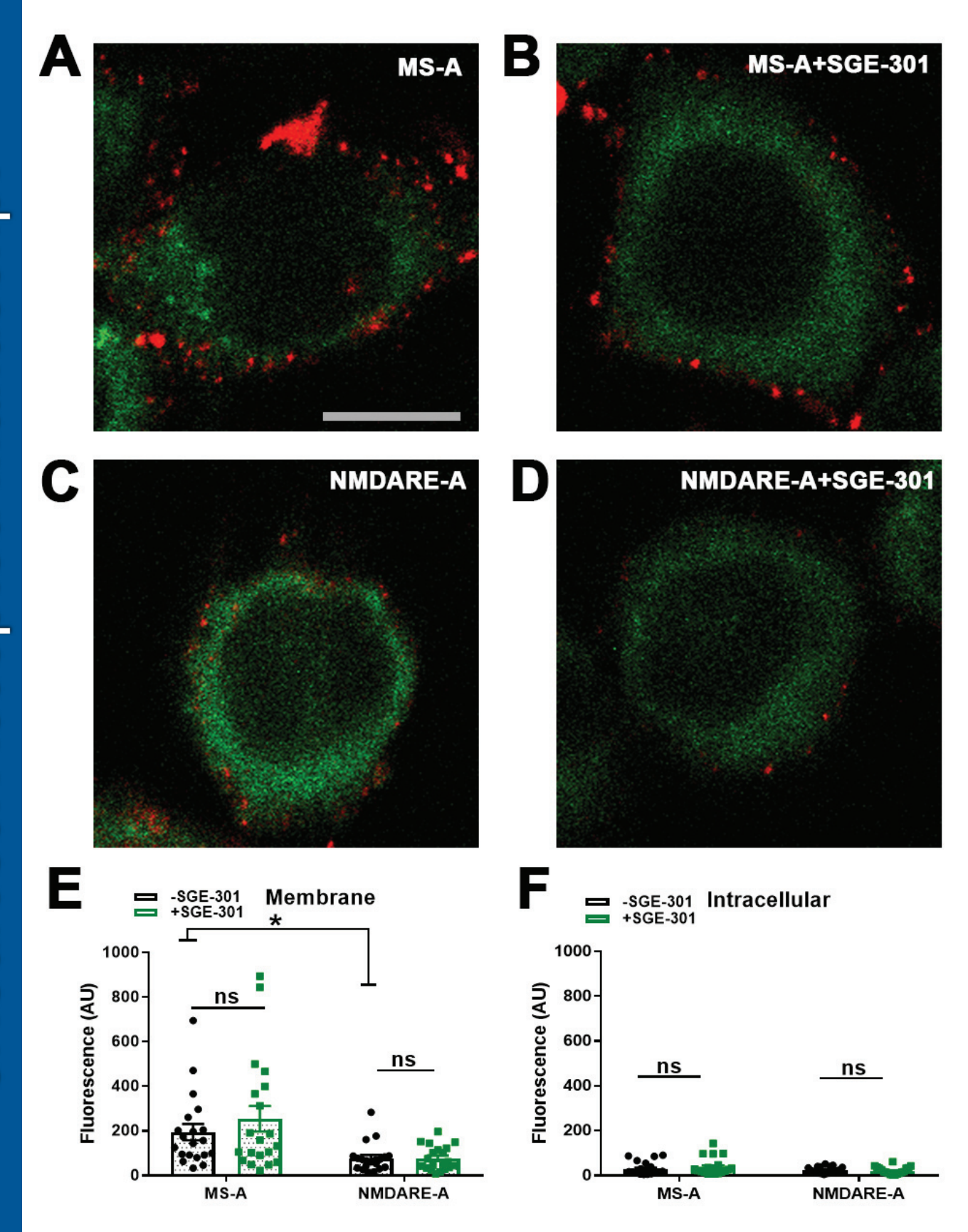






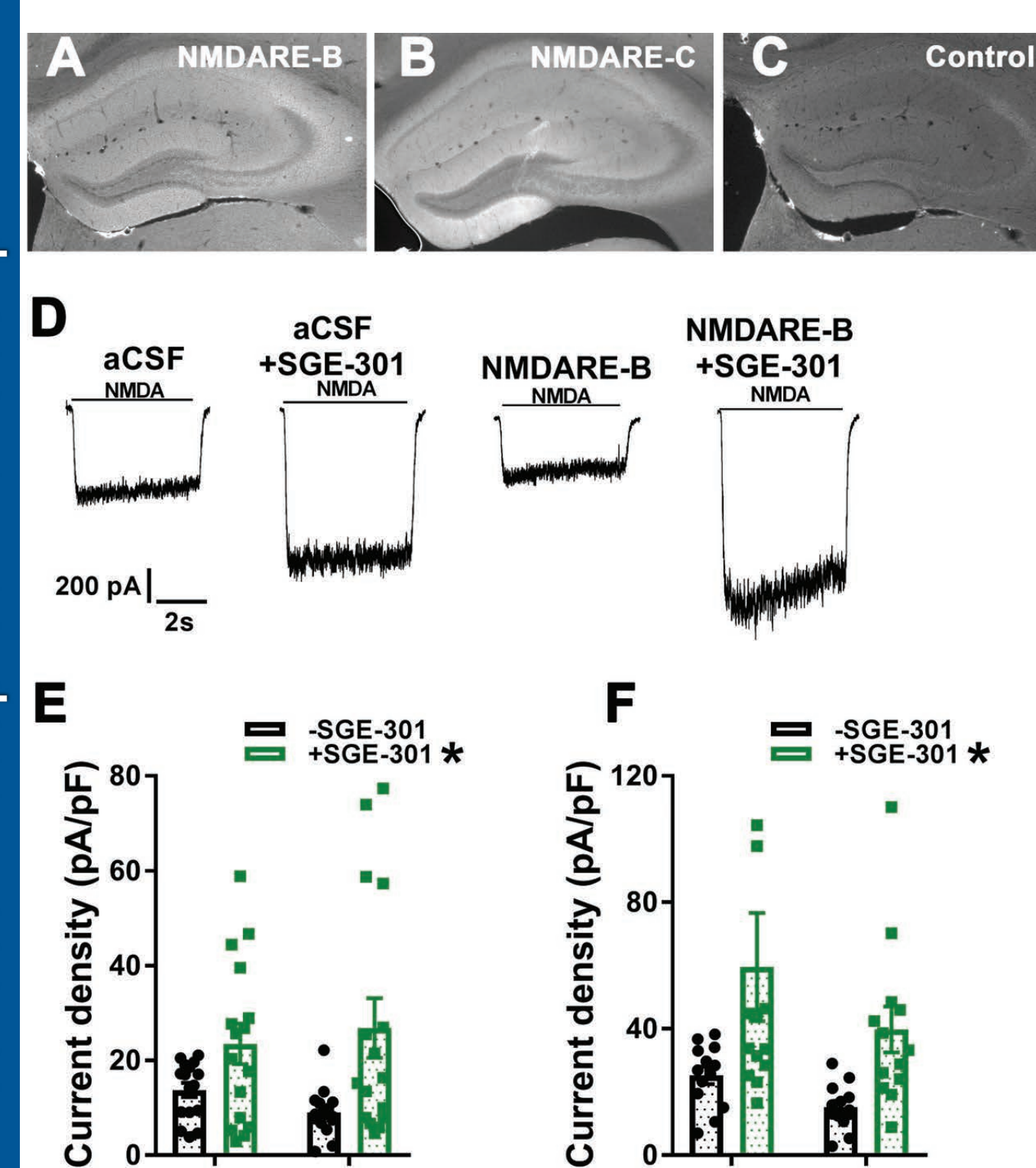






aCSF

NMDARE-B



aCSF

NMDARE-C